Inorganic Chemistry

ARTICLE

pubs.acs.org/IC

The Chemistry of Cadmium−Thiocarboxylate Derivatives: Synthesis, Structural Features, and Application As Single Source Precursors for Ternary Sulfides

Jyotsna Chaturvedi,[†,§] Suryabhan Singh,[†] Subrato Bhattacharya,[*,†] and Heinrich Nöth[‡]

[†]Department of Chemistry, Banaras Hindu University, Varanasi 221005, India

[‡]Department of Chemistry, University of Munich, Butenandtstrasse 5-13, 81377 Munich, Germany

Supporting Information

ABSTRACT: Novel heterobimetallic complexes $[(PPh_3)_2Cu(\mu\text{-}SCOPh)_2Cd(SCOPh)]$ (**2a**), $[(PPh_3)_2Cu(\mu\text{-}SCOth)_2Cd(SCOth)]$ (**2b**), $[(PPh_3)_2Ag(\mu\text{-}SCOth)_2Cd(SCOth)]$ (**3a**), $[(PPh_3)_2Ag(\mu\text{-}SCOth)_2Cd(H_2O)(SCOth)]$ (**3b**), $[(PPh_3)_2Ag(\mu\text{-}SCOPh)_2Cd(SCOPh)]$ (**3c**), and a bimetallic complex $[PPh_3Cd(\mu\text{-}SCOth)SCOth]_2\cdot CH_2Cl_2$ (**5**) (th = thiophene) were prepared and characterized by single crystal X-ray diffraction analysis. A coordination polymer $[Cd(SCOPh)_2]_n$ (**4**) has also been characterized structurally that exhibited metal-like electrical conductivity. The heterobimetallic complexes on pyrolyzing under controlled conditions yielded ternary sulfides of composition $CuCd_7S_8$, $CuCd_{10}S_{11}$, $Ag_2Cd_8S_9$, and $Ag_2Cd_5S_6$, which have been characterized by SEM-EDX and X-ray diffractometry. Photophysical properties and electrical conductivities of the sulfides have also been studied.

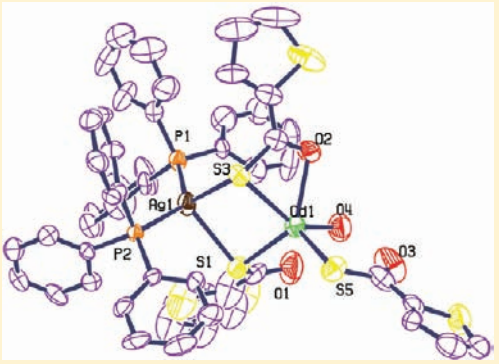

INTRODUCTION

Over the years, metal sulfides in the forms of powders, thin films, and nanoclusters have generated a great deal of scientific and technological interest for different reasons. A number of transition metal sulfides exhibit semiconductivity and other interesting properties like luminescence, photoconductivity, chemical sensing, catalysis, superconductivity, etc.[1] For example, cadmium sulfide is a direct band gap semiconductor (band gap 2.42 eV), and its conductivity increases when irradiated with light, leading to uses as a photoconductor.[2] Cadmium sulfide has two crystalline forms: the more stable hexagonal one has a wurtzite structure, and the cubic form has a zinc blende structure. Both polymorphs are piezoelectric, while the hexagonal form is also pyroelectric.[3] When an impurity (*p*-type semiconductor) is added, it forms the core component of a photovoltaic cell. A CdS/Cu_2S solar cell was one of the first efficient cells known.[4] Furthermore, CdS luminesces under electron beam excitation when doped with Cu^+ and Al^{3+} and is used as a phosphor.[5]

Though a wide variety of methods have been developed to synthesize these materials,[6] the conventional solid state reaction and homogeneous precipitation methods suffer from difficulties like high temperature requirements, long reaction times, the formation of impure products, mixed phases, etc.[7] An attractive method is the single molecular source approach, where the organic fragments present in the metal complexes of sulfur-containing ligands are removed and metal sulfides are reassembled at relatively low temperatures under mild conditions.[8] With the increased complexity of electronic devices, the demand for elegant precursors to deliver complex phases is ever increasing.[9] Metal thiocarboxylates undergo facile thiocarboxylic anhydride elimination, leaving the metal sulfide.[10] Hampden-Smith et al. have shown that the metal thiocarboxylates can be used as single molecular precursors for metal sulfide materials.[11] During recent years, Vittal and Ng developed single-precursor routes to synthesize several sulfide and selenide thin films. They have synthesized a number of thiocarboxylate complexes and exploited them to prepare corresponding metal sulfides. For example, complexes such as $[\{M(SC\{O\}R)_2(bpy)\}]$ (M = Zn, Cd; R = Me/Ph) were utilized to prepare corresponding metal sulfides (cubic ZnS and cubic CdS), and heterobimetallic complexes such as $[(Ph_3P)_2MM'(SC\{O\}Ph)_4]$ (M = Cu, Ag; M′ = In/Ga) were used to prepare binary β-In_2S_3 as well as ternary, $MM'S_2$-type sulfides.[12]

We report here the synthesis and molecular structures of novel heterobimetallic thiocarboxylates containing Cd(II)/Cu(I) and Cd(II)/Ag(I) atoms and the results of studies related to their thermal decomposition into ternary sulfides. The importance of such studies lies in the fact that inclusion of transition metals is known to create intermediate energy states between valence and conduction bands of the CdS crystallites, resulting in a smaller band gap and new optical properties.[13] A lot of studies have so far been conducted using Mn as a dopant, while the study of Cu doping is yet in a nascent state.[14] To the best of our knowledge, a Cd/Ag sulfide is still unknown.

Received: May 3, 2011
Published: September 20, 2011

dx.doi.org/10.1021/ic200927w | *Inorg. Chem.* 2011, 50, 10056–10069

EXPERIMENTAL SECTION

All of the reactions were carried out under a dinitrogen atmosphere. The solvents were purified using standard methods.[15] Cadmium chloride ($CdCl_2 \cdot 2.5H_2O$) (CDH), thiophene-2-carbonyl chloride, and triphenyl phosphine (Sigma-Aldrich) were used as received. Thiobenzoic acid (98%) (Sigma-Aldrich) was purified by distillation (bp 85−87 °C/10 Torr) prior to its use. Thiophene-2-thiocarboxylic acid was synthesized by literature methods.[16] The sodium salt of thiophene-2-thiocarboxylic acid was obtained by reacting the acid with sodium methoxide in a stoichiometric ratio.

IR spectra were recorded using a Varian-3100 FTIR instrument. NMR spectra were obtained using a JEOL AL300 FT NMR spectrometer. Elemental analyses were performed using an Exeter model E-440 CHN analyzer, and electronic absorption spectra were recorded using a Shimazdu UV-1700 PhermaSpec Spectrophotometer.

Synthesis of $[PPh_4]$ $[Cd(SCOth)_3]$ (1). To a stirred solution of sodium thiophene-2-thiocarboxylate (0.210 g, 1.26 mmol) in 5 mL of methanol was added powdered $CdCl_2 \cdot 2.5H_2O$ (0.096 g, 0.42 mmol). The reaction mixture was stirred for half an hour. To the resulting yellow solution was added a solution of tetraphenylphosphonium bromide (0.176 g, 0.42 mmol) in 5 mL of methanol. After 5 min of stirring, a dark yellow precipitate was formed. The precipitate was filtered and dried under reduced pressure and redissolved in a mixture of chloroform and acetonitrile (5:1). After two days, orange crystals suitable for X-ray diffraction were obtained. Yield: 0.307 g (83%). Anal. calcd for $C_{39}H_{29}O_3PS_6Cd$: C, 51.26; H, 3.35. Found: C, 50.87; H, 3.34. IR spectra (KBr, cm^{-1}): 1510 ν(CO), 1224 ν(th-C), 927, 889 ν(C−S). NMR (DMSO-d^6, δ ppm), ^{1}H: 7.04−7.98 (Ph and th ring).^{13}C: 117.05−148.14 (Ph and th ring), 193.88 (COS).

Synthesis of $[(PPh_3)_2Cu(\mu\text{-}SCOPh)_2Cd(SCOPh)]$ (2a). To a methanolic solution (5 mL) of PhCOSH (0.414 g, 3 mmol) was added NaOMe [generated *in situ* by dissolving Na (0.069 g, 3 mmol) metal in 5 mL of methanol] with stirring in an ice bath. After 5 min, a solution of $CdCl_2 \cdot 2.5H_2O$ (0.228 g, 1.00 mmol) in 5 mL of water was added to the reaction mixture, which was then stirred for ∼20 min. To the yellow colored solution was added a solution of $(PPh_3)_2CuNO_3$ (0.650 g, 1.00 mmol) in 5 mL of CH_2Cl_2, and the solution was stirred for an hour. The solvent was evaporated under reduced pressure, and the residue was extracted with chloroform, which on layering with diethyl ether yielded crystals of **2a** after 3 days. Yield: 1.024 g (92%). Anal. calcd for $C_{57}H_{45}O_3P_2S_3CdCu$: C, 61.56, H, 4.08. Found: C, 61.31, H, 4.04. IR spectra (KBr, cm^{-1}): 1591, 1545 ν(CO), 1207 ν(Ph−C), 933 ν(C−S). NMR ($CDCl_3$, δ ppm): ^{1}H, 7.14−7.76 (Ph).^{13}C, 127.50−139.13 (Ph), 206.93 (COS).^{31}P, 2.25.

Synthesis of $[(PPh_3)_2Cu(\mu\text{-}SCOth)_2Cd(SCOth)]$ (2b). To a stirred solution of sodium thiophene-2-thiocarboxylate (0.298 g, 1.80 mmol) in 10 mL of methanol was added powdered $CdCl_2 \cdot 2.5H_2O$ (0.137 g, 0.60 mmol). After stirring the reaction mixture for 15 min, a solution of $(PPh_3)_2CuNO_3$ (0.390 g, 0.60 mmol; in 5 mL of CH_2Cl_2) was added dropwise into it. The reaction mixture was stirred further for an hour; then it was dried under reduced pressure. The yellow residue was then redissolved in toluene, and after removing the NaCl, the solution was kept for crystallization. After a day, pale yellow crystals were obtained. Yield: 0.563 g (83%). mp 144−146 °C. Anal. calcd for $C_{51}H_{39}O_3P_2S_6CdCu$: C, 54.20; H, 3.48. Found: C, 54.19; H, 3.46. IR spectra (KBr, cm^{-1}): 1543, 1510 ν(CO), 1228 ν(th-C), 918, 879 ν(C−S). NMR ($CDCl_3$, δ ppm), ^{1}H: 6.82−7.57 (Ph and th). ^{13}C: 127.34−145.57 (Ph and th), 197.69 (COS). ^{31}P: 2.07.

Synthesis of $[(PPh_3)_2Ag(\mu\text{-}SCOth)_2Cd(SCOth)]$ (3a) and $[(PPh_3)_2Ag(\mu\text{-}SCOth)_2Cd(SCOth)H_2O]$ (3b). The same procedure was followed as mentioned for **2b** except the fact that $(PPh_3)_2AgNO_3$ (0.361 g, 0.52 mmol) was used in place of $(PPh_3)_2CuNO_3$. Yield: 0.476 g (78%). A closer look into the product revealed the presence of two types of crystals.

Type 1 (**3a**): Block -shaped yellow crystals. mp 166−168 °C. Anal. cald for $C_{51}H_{39}O_3P_2S_6AgCd$: C, 51.26; H, 3.35. Found: C, 50.87; H, 3.34. IR spectra (KBr, cm^{-1}): 1575, 1545 ν(CO), 1226 ν (th-C), 916, 895 ν(C−S). NMR ($CDCl_3$, δ ppm), ^{1}H: 6.89−7.70 (Ph and th). ^{13}C: 127.28−145.70 (Ph and th), 197.64 (COS). ^{31}P: 10.40.

Type 2 (**3b**): Block-shaped pale yellow crystals. mp 172−174 °C. Elemental analysis, anal. calcd for $C_{51}H_{41}O_4P_2S_6AgCd$: C, 51.37; H, 3.47. Found: C, 51.23; H, 3.45. IR (KBr, cm^{-1}): 1583 ν(CO), 1224 ν(th-C), 905, 870 ν(C−S). NMR ($CDCl_3$, δ ppm), ^{1}H: 6.78−7.55 (Ph and th), 2.35 (H_2O).^{13}C: 127.29−145.66 (Ph and th), 197.69 (COS). ^{31}P: 10.47.

Synthesis of $[(PPh_3)_2Ag(\mu\text{-}SCOPh)_2Cd(SCOPh)]$ (3c). The same procedure was followed as mentioned in the case of **2a** except in place of $(PPh_3)_2CuNO_3$, $(PPh_3)_2AgNO_3$ (0.382 g, 0.55 mmol) was used. Block-shaped, colorless crystals suitable for single crystal X-ray diffraction were obtained from a toluene solution. Yield: 0.59 g (93%). mp 164 − 166 °C. Anal. calcd for $C_{57}H_{45}O_3P_2S_3AgCd$: C, 59.20; H, 3.92. Found: C, 58.97; H 3.90. IR (KBr, cm^{-1}): 1569 ν(CO), 1214 ν(Ph−C), 938 ν(C−S). NMR ($CDCl_3$, δ ppm), ^{1}H: 7.11−7.89 (Ph). ^{13}C: 127.48−139.12 (Ph), 206.79 (COS). ^{31}P: 9.49.

Synthesis of $[Cd(SCOPh)_2]_n$ (4). *Method A (Using $TiCl_4$).* To a stirred solution of NaSCOPh prepared *in situ* by reacting thiobenzoic acid (0.414 g, 3 mmol) and sodium metal (0.069 g, 3 mmol) in MeOH (15 mL) was added an aqueous solution (5 mL) of $CdCl_2 \cdot 2.5H_2O$ (0.228 g, 1 mmol) to get a yellow-colored solution of $Na[Cd(SCOPh)_3]$. A solution of $TiCl_4$((0.047 g, 0.25 mmol) in MeOH (10 mL) was then added to the reaction mixture with vigorous stirring at 10 °C. Stirring was continued for 1 h at room temperature. The solvent was then evaporated under reduced pressure, and the residue was extracted with $CHCl_3$ (20 mL). The material was filtered off, and solvent from the filtrate was evaporated under reduced pressure. The yellow-colored crystalline product was washed with ethanol to remove the dibenzoyl disulfide. After recrystallization from a chloroform and acetonitrile mixture (1:1), the product was dried under vacuum conditions for 1 h. Single crystals of the compound obtained were very thin, needle like, and of poor quality. Yield, based on $CdCl_2$: 0.368 g (95.2%). mp 165 °C. Anal. calcd for $C_{14}H_{10}O_2S_2Cd_1$: C, 43.48; H, 2.61. Found: C, 43.80; H, 2.70. IR data (KBr, cm^{-1}): 1545 ν(CO), 1221 ν (Ph−C), 943 ν (C−S), 632. NMR ($CDCl_3$, δ ppm), ^{1}H: 7.09−7.78 (Ph). ^{13}C: 127−132.6 (Ph), 200.5 (COS).

Method B (Using MgO). To a stirred solution of thiobenzoic acid (0.414 g, 3.0 mmol) in 5.0 mL of methanol was added a suspension of MgO (0.060 g, 1.50 mmol) in MeOH (15 mL) followed by an aqueous solution (5 mL) of $CdCl_2 \cdot 2.5H_2O$ (0.228 g, 1 mmol), resulting in a yellow-colored turbid solution, which was stirred further for 1 h at room temperature. The solvent was then evaporated under reduced pressure, and the residue was extracted with a methanol and acetonitrile (1:1) mixture. The insoluble material was filtered off, and on standing, yellow-colored crystals were obtained in a few days. Yield (based on $CdCl_2 \cdot 2.5H_2O$): 0.368 g (95.0%). mp 165 °C. Anal. calcd for $C_{14}H_{10}O_2S_2Cd_1$: C, 43.48; H, 2.61. Found: C, 43.60; H, 2.68. IR data (KBr, cm^{-1}): 1545 ν(CO), 1221 ν(Ph−C), 943 ν(C−S). NMR ($CDCl_3$, δ ppm), ^{1}H: 7.09−7.78 (Ph). ^{13}C: 127−132.6 (Ph), 200.5 (COS).

Synthesis of $[PPh_3Cd(\mu\text{-}SCOth)SCOth]_2 \cdot CH_2Cl_2$ (5). To a stirred solution of sodium thiophene-2-thiocarboxylate (0.210 g, 1.27 mmol) in 5 mL of methanol was added $CdCl_2 \cdot 2.5H_2O$ (0.145 g, 0.63 mmol), followed by a CH_2Cl_2 solution of PPh_3 (0.166 g, 0.63 mmol). The reaction mixture was stirred for 2 h and then was dried under reduced pressure. The residue was dissolved in chloroform and filtered off NaCl. The filtrate was layered with petroleum ether (60−80 °C fraction), which on standing yielded colorless crystals after a day. Yield: 0.375 g (84%). mp 182−84 °C. Anal. calcd for $C_{57}H_{44}Cl_2O_4P_2S_8Cd_2$: C, 48.65; H, 3.15. Found: C, 48.45; H, 3.13. NMR ($CDCl_3$, δ ppm), ^{1}H: 6.93−7.75 (Ph and th). ^{13}C: 127.62−145.40 (Ph and th), 198.15 (COS).

dx.doi.org/10.1021/ic200927w |*Inorg. Chem.* 2011, 50, 10056–10069

Table 1. Crystal Data and Structure Refinement of 1−5

	1	2a	2b	3a	3b	3c	4	5
empirical formula	$C_{39}H_{29}Cd_1O_3P_1S_6$	$C_{57}H_{45}Cd_1Cu_1O_3P_2S_3$	$C_{51}H_{38.75}Cd_1Cu_1O_3P_2S_6$	$C_{51}H_{39}Cd_1Ag_1O_3P_2S_6$	$C_{51}H_{41}Cd_1Ag_1O_4P_2S_6$	$C_{57}H_{45}Cd_1Ag_1O_3P_2S_3$	$C_{56}H_{40}Cd_4O_8S_8$	$C_{58}H_{46}Cd_2O_4P_2S_8Cl_4$
M	881.42	1112.04	1129.81	1174.46	1192.48	1156.36	1547.08	1492.07
T/K	100(2)	293(2)	293(2)	293(2)	293(2)	293(2)	293(2)	293(2)
cryst syst	trigonal	monoclinic	monoclinic	monoclinic	orthorhombic	monoclinic	triclinic	triclinic
space group	$P32$	$P21/n$	$P21/n$	$P21$	$Pccn$	$P21$	$P\bar{1}$	$P\bar{1}$
a/Å	12.8884(5)	12.6333(4)	12.660(5)	12.6836(3)	13.9235(5)	12.7887(2)	11.2551(7)	11.016(5)
b/Å	12.8884(5)	17.7820(6)	17.532(5)	14.5643(2)	39.2078(18)	14.7387(2)	14.2713(9)	12.676(5)
c/Å	19.6867(9)	23.0121(8)	22.631(5)	14.3913(3)	18.1192(5)	14.1904(3)	17.7941(11)	12.956(5)
α/deg	90	90	90.000(5)	90	90	90	82.502(5)	71.529(5)
β/deg	90	96.631(3)	95.538(5)	107.029(2)	90	107.071(2)	89.949(5)	68.282(5)
γ/deg	120	90	90.000(5)	90	90	90	78.471(6)	87.580(5)
V/Å^3	2832.1(2)	5135.0	5000(3)	2541.92(9)	9891.5(6)	2556.89(8)	2775.6(3)	1588.4(11)
Z	3	4	4	2	8	2	2	1
μ (mm^{-1})	0.990	1.056	1.207	1.154	1.188	1.028	1.867	1.195
final R indices [$I > 2\sigma(I)$]	R1 = 0.0338	R1 = 0.0568	R1 = 0.0807	R1 = 0.0393	R1 = 0.0991	R1 = 0.0229	R1 = 0.0591	R1 = 0.0458
	wR2 = 0.0788	wR2 = 0.1527	wR2 = 0.1840	wR2 = 0.0881	wR2 = 0.2159	wR2 = 0.0420	wR2 = 0.1440	wR2 = 0.1225
R indices (all data)	R1 = 0.0429	R1 = 0.0889	R1 = 0.1346	R1 = 0.0592	R1 = 0.1556	R1 = 0.0293	R1 = 0.0987	R1 = 0.0680
	wR2 = 0.0813	wR2 = 0.1653	wR2 = 0.2222	wR2 = 0.0933	wR2 = 0.2343	wR2 = 0.0430	wR2 = 0.1724	wR2 = 0.1322
GOF on F^2	1.014	1.085	1.037	0.922	1.045	0.950	1.040	1.075
largest diff. peak and hole	0.427 and −0.731	2.223 and −0.798	1.449 and −1.129	0.727 and −0.864	1.680 and −1.640	0.284 and −0.323	1.875 and −0.865	1.630 and −0.722

dx.doi.org/10.1021/ic200927w |*Inorg. Chem.* 2011, 50, 10056–10069

X-Ray Crystallography. Single crystal X-ray data of compounds **1**−**5** were collected on an Xcalibur Eos Oxford Diffractometer using graphite monochromated Mo Kα radiation (λ = 0.7107 Å). Data collections for **1** were carried out at 100 K, while those for **2a**, **2b**, **3a**, **3b**, **3c**, **4**, and **5** were carried out at 293 K. Absorption corrections were made using the multiscan method. Data integration and reductions were processed with CRYSALIS PRO software.[17] Structures were solved by the direct method and then refined on F^2 using the full matrix least-squares technique with SHELX-97 software[18] using the WINGX program package.[19] Hydrogen atoms were, however, placed at the calculated positions using SHELX default parameters. Disordered atoms were split into two parts and then refined with free variables using appropriate restraints. A summary of crystallographic data and structure solutions are given in Table 1.

Powder X-ray diffraction scans were obtained using a Bruker Powder X- Ray Diffractometer with a Cu target (λ = 1.54056 Å).

Thermogravimetry and Pyrolysis. Thermogravimetric analyses were carried out using a Perkin-Elmer Diamond TG/DTA with a heating rate of 10 °C min^{-1} under an argon atmosphere. Pyrolyses of the compounds in the solid state were performed at 350 °C in a furnace which was continuously purged with dry N_2 gas. The residue obtained in each case was a mixture of different compounds from which metal sulfides were isolated by washing the residue successively with ethanol, diethyl ether, and carbon disulfide. The suspended particles were collected by centrifugation and were then dried under vacuum conditions and 0.1 mmHg/2 h. We have not tried to analyze the soluble compounds fully. However, elemental sulfur was obtained on drying the carbon disulfide solution, while the presence of Cu^{2+}/Ag^{+} ions was detected qualitatively, and crystals of triphenylphosphine oxide were obtained on drying the ethanol and diethyl ether solutions respectively.

SEM-EDS Analysis. Scanning electron microscopic images were taken on a JEOL model JSM-6390LV, while energy dispersive X-ray spectrometric data were taken on a JEOL model JED-2300.

Photoluminescence (PL) Spectra and Photoluminescence Excitation Spectra (PLE). Spatially resolved PL spectra were collected using a WItec Alpha SNOM (Germany; Scanning Near-field Optical Microscope) in confocal mode in transmission geometry from different regions of the sample which was a thin film on a glass substrate. The samples were excited by an argon laser (λ = 488 nm) through an OIL immersion objective lens (100×) with a numerical aperture (NA = 0.95). The PL spectra were collected using CCD with a spectral grating of 150 g/mm and an integration time of 5 s at excitation powers of 0.1 and 0.3 mW of the 488 nm laser used.

Pressed Pellet Electrical Conductivity. The pressed pellet electrical conductivity of complex $[Cd(SCOPh)_2]_n$ and ternary metal sulfides $CuCd_7S_8$, $CuCd_{10}S_{11}$, and $Ag_2Cd_5S_6$ were recorded on a Kiethley-236 source measurement unit by employing a conventional two-probe technique.

RESULTS AND DISCUSSION

Syntheses. The sodium salt of the complex $[Cd(SCOR)_3]^-$ was generated *in situ*, which on exchange of the cation yielded the complexes **1**−**4**, as shown in Scheme 1. Notably, the reaction of *bis*-triphenyl phosphinesilver(I) nitrate with $Na[Cd(SCOth)_3]$ resulted in two different kinds of crystals with different coordination environments around the Cd(II) centers: one containing $[(PPh_3)_2Ag(SCOth)_2Cd(SCOth)]$ (**3a**) formula units in which Cd(II) is surrounded by three thiocarboxylate units and the other having the formula $[(PPh_3)_2Ag(SCOth)_2Cd(H_2O)(SCOth)]$ (**3b**), in which there is a water molecule coordinated to Cd(II). The analogous reaction with $Na[Cd(SCOPh)_3]$ gave only one product, $[(PPh_3)_2Ag(SCOPh)_2Cd(SCOPh)]$ (**3c**). It is worth mentioning here that there are only a few heterobinuclear Cd(II)/Cu(II) complexes known[20] to date, while complexes of Cd(II)/Cu(I) and Cd(II)/Ag(I) containing a sulfur ligand are hitherto unknown.

Scheme 1

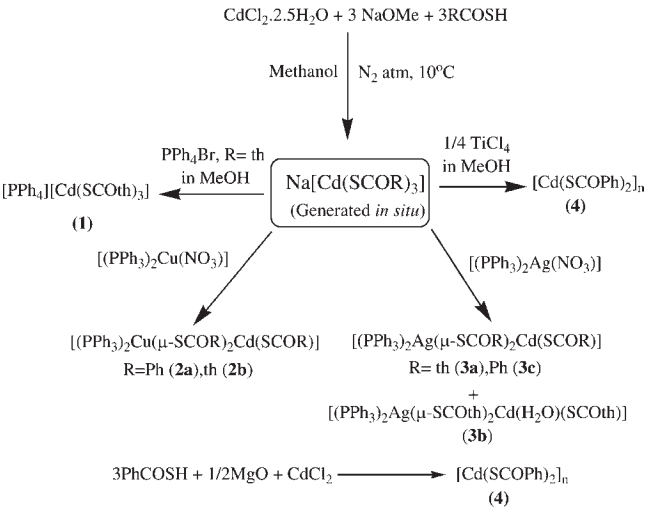

Scheme 2

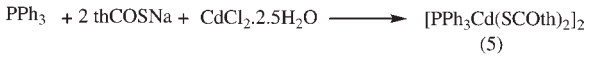

Though the Na^+ ion could easily be exchanged with other large cations (in complexes **1**−**3**) which are of a soft nature, an attempt to replace the same with a hard metal ion such as Ti^{4+} did not yield the expected heterobinuclear complexes. Instead, the binary thiocarboxylate of Cd(II) was isolated. A similar result was obtained when an attempt was made to isolate the magnesium salt of the complex $[Cd(SCOR)_3]^-$. Very recent studies on analogous Zn(II) complexes showed migration of a phosphine ligand from Cu(I) to Zn(II) during the formation of a heterobinuclear complex.[21] Such ligand migration was observable in none of the Cd(II) complexes during the present studies. However, binding of phosphine is quite facile with Cd(II) in its thiocarboxylate complex, as shown in Scheme 2.

All of the complexes were found to be stable at ambient temperature for several months.

Crystal and Molecular Structures. Complex **1** crystallized in the trigonal system with space group $P3_2$ as discrete cation−anion pairs. In the anionic part, Cd(II) is hexacoordinated by three oxygen and three sulfur atoms. The geometry around Cd(II) is between trigonal prismatic and trigonal antiprismatic with a twist angle (ϕ) of 27.6° (Figure 1). Though the anion of **1** is structurally comparable to $[Cd(SCOPh)_3]^-$, the Cd···O distances in **1** are significantly shorter than those found in the latter complex[22] (2.659−2.828 Å).

The complex (**2a**) crystallized in the monoclinic system with the $P2_1/n$ space group. The thermal ellipsoid plot is shown in Figure 2. The Cd−Cu distance 3.577 Å is quite larger than the sum of the covalent radii of the two metals (2.86 Å). The known Cd(II)/Cu(II) heterodinuclear complexes are $[Cd_2Cu_2I_4L_4(DMSO)_2]$,

dx.doi.org/10.1021/ic200927w |*Inorg. Chem.* 2011, 50, 10056–10069

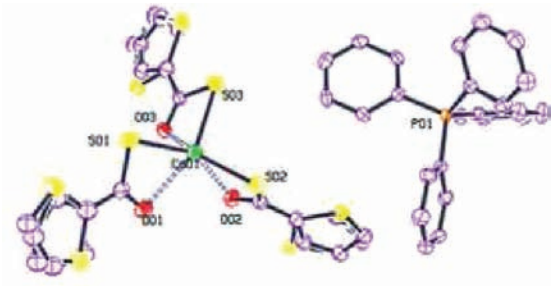

Figure 1. Thermal ellipsoid plot (at 50% probability level) of **1**. The thiophene rings are disordered. Hydrogen atoms are omitted for clarity. Selected metric data: Cd−S(1) 2.547(13), Cd−S(2) 2.564(13), Cd−S(3) 2.610(13), Cd−O(1) 2.560(4), Cd−O(2) 2.487(3), Cd−O(3) 2.431(3). S(1)−Cd−S(2) 122.72(4), S(1)−Cd−S(3) 105.58(4), S(2)−Cd−S(3) 107.09(4), O(1)−Cd−O(2) 86.84(11), O(1)−Cd−O(3) 92.39(11), O(2)−Cd−O(3) 85.95(11), S(1)−Cd−O(1) 60.93(8), S(1)−Cd−O(3) 92.48(8), S(1)−Cd−O(2) 147.67(8), S(2)−Cd−O(1) 100.72(8), S(2)−Cd−O(2) 62.34(8), S(2)−Cd−O(3) 144.53(8), S(3)−Cd−O(1) 151.87(9), S(3)−Cd−O(2) 102.17(8), S(3)−Cd−O(3) 62.23(8).

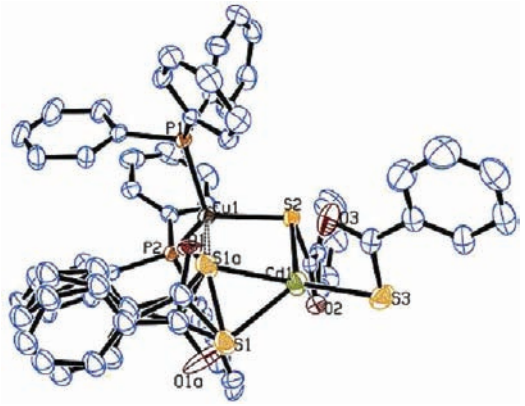

Figure 2. Thermal ellipsoid plot (at 30% probability level) of **2a**. Hydrogen atoms have been omitted for clarity. Selected metric data: Cd−S(3) 2.493(1), Cd−S(2) 2.572(1), Cd−S(1) 2.529(3), Cd−S(1a) 2.498(4), Cd−O(3) 2.592(4), Cd−O(2) 2.607(3), Cu−P(2) 2.264(1), Cu−P(1) 2.286(1), Cu−S(2) 2.353(1), Cu−O(1) 2.381(9), S(2)−C(44) 1.769(5), S(3)−C(51) 1.747(6), S(1)−C(37) 1.673(19), O(1)−C(37) 1.265(15), O(2)−C(44) 1.231(6), O(3)−C(51) 1.232(6), P(1)−C(13) 1.820(5), P(1)−C(1) 1.825(4), P(1)−C(7) 1.826(5), P(2)−C(19) 1.818(5), P(2)−C(31) 1.821(5), P(2)−C(35) 1.830(5). S(3)−Cd−S(2) 116.25(6), S(3)−Cd−S(1) 144.26(8), S(2)−Cd−S(1) 85.81(7), S(3)−Cd−O(1) 119.97(8), O(1)−Cd−S(2) 123.36(8), O(1)−Cd−S(1) 51.26(10), S(2)−Cd−O(3) 93.76(11), O(1)−Cd−O(2) 102.96(12), O(3)−Cd−S(1) 91.64(11), S(1)−Cd−O(2) 115.94(10), O(3)−Cd−O(2) 138.33(14), S(2)−Cd−O(2) 60.33(14), S(3)−Cd−O(2) 99.68(9), P(2)−Cu−S(2) 116.95(5), P(2)−Cu−P(1) 121.35(5), P(2)−Cu−S(1) 115.47(7), P(1)−Cu−S(2) 107.55(5), S(2)−Cu−S(1) 90.71(8), P(1)−Cu−S(1) 99.43(9), C(44)−S(2)−Cu 109.34(14), Cu−S(2)−Cd 93.02(5).

$[Cd_2Cu_3Br_6L_4(DMSO)_2]$, and $[Cd_4Cu_2Cl_6L_6(H_2O)_2]$ (where LH = 2-dimethylaminoethanol),[20] in which the M−M distances vary from 3.399 to 4.043 Å and no M−M bond has been considered while describing the structures. As mentioned already, **2a** and **2b** are the first Cd(II)/Cu(I) heterodinuclear complexes, and there are no structural data available for further comparison of the Cd(II)−Cu(I) distance.

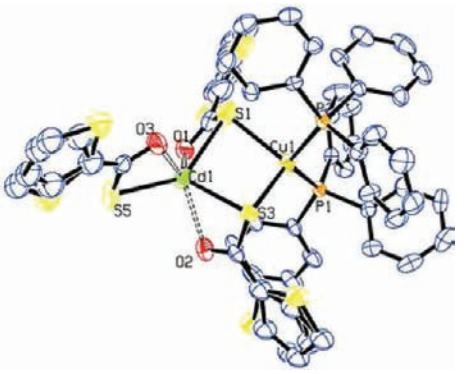

Figure 3. Thermal ellipsoid plot (at 30% probability level) of **2b** with disordered thiophene rings (hydrogen atoms are omitted for clarity). Selected metric data: Cd−S(1) 2.608(3), Cd−S(3) 2.594(2), Cd−S(5) 2.478(2), Cd−O(1) 2.618(7), Cd−O(2) 2.575(6), Cu−P(1) 2.292(1), Cu−P(2) 2.292(1), Cu−S(1) 2.583(3), Cu−S(3), 2.380(1). S(3)−Cd−S(1) 90.23(7), S(5)−Cd−S(1) 139.02(9), S(5)−Cd−S(3) 120.42(8), O(2)−Cd−O(1) 91.67(19), S(5)−Cd−O(2) 99.95(14), S(3)−Cd−O(2) 60.47(13), S(1)−Cd−O(2) 119.65(13), S(5)−Cd−O(1) 115.29(15), S(3)−Cd−O(1) 120.48(14), S(1)−Cd−O(1) 57.51(15), P(1)−Cu−P(2) 120.97(6), P(1)−Cu−S(3) 115.18(7), P(1)−Cu−S(1) 118.76(8), P(2)−Cu−S(3) 105.35(7), P(2)−Cu−S(1) 96.57(9), S(3)−Cu−S(1) 95.79(8).

The three thiocarboxylate ligands display three different bonding modes: bidentate SCO bridging, S-bridging chelating, and chelating (terminal), as shown in Figure 2. Notably, the disordered bridging (μ-S,O) ligand makes it difficult to describe the geometry around the Cd(II) center. The sof of the two parts of a disordred atom are similar (48 and 52%). It is, however, clear that Cd(II) is pentacoordinate and bonded with two oxygen and one sulfur atoms. For pentacoordinate complexes, Addison et al.[23] have given an angular structural parameter, τ, and defined it as an index of trigonality. The value of τ varies from 0 to 1 when the geometry changes from perfect square pyramidal to ideal trigonal bipyramidal. Two τ values were calculated for the structure, one considering the S1 and the other considering the S1A atom bonded to Cd(II). The values obtained (0.23 and 0.09) are indicative of distorted square pyramidal geometry around Cd(II). The Cd−S(3) bond [2.493(1) Å] is shorter than the other two Cd−S bonds in which S atoms are involved in bridging.

Besides the phosphorus atoms of two triphenylphosphine ligands, the Cu(II) is bonded to the sulfur and oxygen atoms of the μ-S and μ-S,O thiobenzoate ligands, respectively. The Cu−S bond length is within the range reported for Cu−S bond lengths in copper thiobenzoate complexes.[24] The bond angles around the Cu center are, however, quite deviated from the ideal value of 109.5° due to steric requirements. Yang et al.[25] have introduced a simple four-coordinate metrical parameter τ_4 to objectively describe the molecular geometry, which is neither close to tetrahedral nor square planar. The τ_4 value for **2a** was found to be 0.86, which is indicative of a trigonal pyramidal geometry.

The molecular structure of the Cd/Cu-containing thiophene-2-thiocarboxylate complex is slightly different from that of **2a**. Two of the three thiocarboxylate groups exhibit a μ-S bridging mode of bonding. As shown in Figure 3, the cadmium atom in **2b** is hexacoordinated and surrounded by three oxygen and three sulfur atoms. Cd is tipped above the O1O2O3 plane by 0.093 Å.

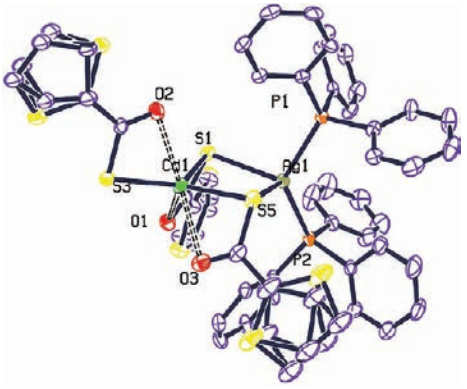

Figure 4. Thermal ellipsoid plot (at 50% probability level) of **3a** with disordered thiophene rings (hydrogen atoms are omitted for clarity). Selected metric data: Cd−S(1) 2.612(13), Cd−S(3) 2.474(1), Cd−S(5) 2.572(1), Cd−O(1) 2.464(4), Cd−O(2) 2.650(4), Cd−O(3) 2.579(4), Ag−P(1) 2.485(1), Ag−P(2) 2.642(12), Ag−S(1) 2.694(12), Ag−S(5) 2.816(1). P(1)−Ag−P(1) 125.31(4), P(1)−Ag−S(1) 104.02(4), P(1)−Ag−S(5) 95.92(4), P(2)−Ag−S(5) 117.69(5), P(2)−Ag−S(1) 116.01(4), S(1)−Ag−S(5) 91.29(4), S(3)−Cd−S(1) 127.66(5), S(5)−Cd−S(1) 120.80(9), S(3)−Cd−S(5) 129.57(5), O(1)−Cd−O(2) 136.39(14), O(1)−Cd−O(3) 79.54(12), O(3)−Cd−O(2) 140.51(13).

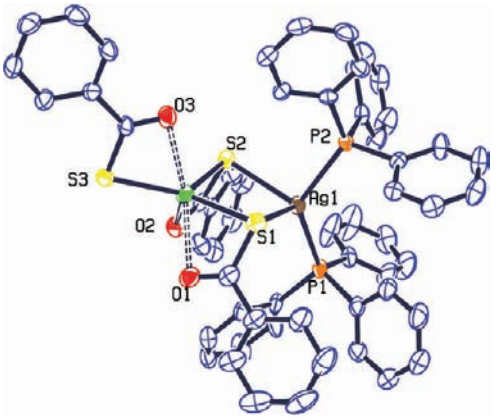

Figure 5. Thermal ellipsoid plot (at 50% probability level) of **3c**. Hydrogen atoms have been omitted for clarity. Selected metric data: Cd−S(1) 2.612(1), Cd−S(3) 2.474(1), Cd−S(5) 2.572(15), Cd−O(1) 2.464(4), Cd−O(2) 2.650(4), Cd−O(3) 2.579(4), Ag−P(1) 2.485(12), Ag−P(2) 2.464(1), Ag−S(1) 2.694(1), Ag−S(5) 2.816(1). P(1)−Ag−P(2) 125.93(2), P(1)−Ag−S(1) 117.00(2), P(1)−Ag−S-(2) 119.48(4), P(2)−Ag−S(1) 98.61(2), P(2)−Ag−S(2) 98.65 (1), S(2)−Ag−S(1) 89.62(1), S(3)−Cd−O(1) 99.89(4), S(3)−Cd−O(2) 102.31(4), O(1)−Cd−O(2) 81.34(6), S(3)−Cd−S(1) 133.98(2), O-(1)−Cd−S(1) 61.02(4), O(2)−Cd−S(1) 114.04(4), S(3)−Cd−S(2) 126.12(12), O(1)−Cd−S(2) 124.12(4), O(2)−Cd−S(1) 61.14(4), S(1)−Cd−S(2) 96.68(2), S(3)−Cd−O(3) 61.22(4), O(1)−Cd−O(3) 135.77(6), O(2)−Cd−O(3) 138.98(6), S(1)−Cd−O(3) 101.87(4), S(2)−Cd−O(3) 96.78(4).

The triangular faces O2O1S5 and S1S3O3 of the approximate trigonal prisms are almost parallel to each other with an interplanar angle of 1.37° with a *meridional* configuration. The coordination environment around the Cu atom is comparable to that observed in **2a** (τ_4 = 0.85). The thiophene rings of terminal thiocarboxylate groups (bonded to Cd) of two adjacent molecules are arranged in a displaced parallel fashion with a centroid−centroid distance of 3.94 Å, indicating $\pi-\pi$ stacking.

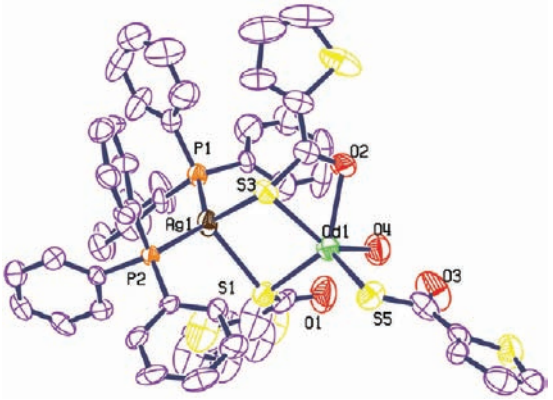

Figure 6. Thermal ellipsoid plot (at 50% probability level) of **3b** with disordered thiophene rings (hydrogen atoms are omitted for clarity). Selected metric data: Cd−S(1) 2.604(3), Cd−S(3) 2.647(3), Cd−S(5) 2.481(3), Cd−O(2) 2.437(7), Cd−O(4) 2.290(9), Ag−P(1) 2.437(3), Ag−P(2) 2.478(2), Ag−S(1) 2.708(3), Ag−S(3) 2.744(3). P(1)−Ag−P(2) 131.51(9), S(1)−Ag−S(3) 88.10(9), P(1)−Ag−S(1) 115.70(9), P(1)−Ag−S(3) 117.53(9), P(2)−Ag−S(1) 101.97(9), P(2)−Ag−S(3) 117.53(9), S(1)−Cd−S(3) 92.42(9), S(1)−Cd−S(5) 113.47(10), S(3)−Cd−S(5) 110.00(10), O(4)−Cd−O(2) 85.4(3), O(4)−Cd−S(1) 94.6(2), O(4)−Cd−S(3) 140.3(3), O(4)−Cd−-S(5) 102.8(2), O(2)−Cd−S(1) 130.5(2), O(2)−Cd−S(3) 61.02(12), O(2)−Cd−S(5) 114.8(2).

A comparison with the reported bimetallic complexes revealed notable structural differences with **2a** and **2b**. Earlier reported anions, $[A\{Cd(SCOPh)_3\}_2]^-$ (where A = Na/K), showed trigonal planar Cd(II) centers bonded to the three sulfur atoms of the ligands.[26] On the other hand, in the Cu(I)-containing complexes $[(Ph_3P)CuM(SCOPh)_4]$ (where M = Ga/In), two of the three thiocarboxylate ligands exhibit a μ-S,O mode of bridging the two atoms.[27]

The heterobimetallic complexes **3a** and **3c** crystallized in a monoclinic system with space group $P2_1$. The thermal ellipsoid plots of **3a** and **3c** are given in Figures 4 and 5. A survey of literature revealed that these are the first examples of Cd/Ag heterobinuclear complexes. The Cd−Ag distances (3.568 and 3.598 Å) in **3a** and **3c** are longer than the sum of the van der Waals radii of Ag and Cd atoms (3.30 Å), and there is no possibility of any bonding interactions between these two metal centers.

In both complexes, Ag(I) is bonded with phosphorus atoms of two triphenylphosphine moieties and two sulfur atoms of the thiocarboxylate ligands. The bond angles subtended at the silver atom are indicative of trigonal pyramidal (τ_4= 0.83 and 0.81 for **3a** and **3c**, respectively) coordination geometry. The Ag−S(5) bond length [2.816 (1)Å] in case **3a** is possibly the longest silver−sulfur bond reported so far (the longest Ag−S bond length reported earlier was 2.735 Å in $[(AgPPh_3)_4(\mu$-SC{O}Ph-*S*)4]).[28]

In both **3a** and **3c**, the Cd(II) is hexacoordinated and is surrounded by three oxygen and three sulfur atoms. The two triangular faces are almost parallel to each other in both cases with interplanar angles of 0.74° and 1.03° respectively in **3a** and **3c**. As observed in **2a** and **2b**, the terminal Cd−S distances are shorter than the bridging Cd−S bonds.

Complex **3b** crystallized in the triclinic system with the $P\bar{1}$ space group. The Cd(II) center (Figure 6) is four coordinated

dx.doi.org/10.1021/ic200927w |*Inorg. Chem.* 2011, 50, 10056–10069

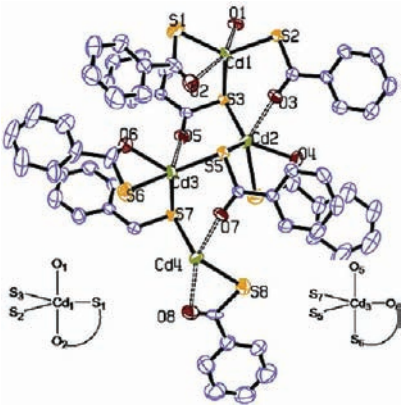

Figure 7. Thermal ellipsoid plot of complex **4** (at 50% probability). Hydrogen atoms are omitted for the clarity. Stereochemistries of Cd1 and Cd3 have been shown schematically. Selected metric data: Cd(1)−O(1) 2.516(4), Cd(1)−O(2) 2.546(5), Cd(1)−S(1) 2.492(2), Cd(1)−S(2) 2.512(1), Cd(1)−S(3) 2.579(1), Cd(2)−S(3) 2.498(1), Cd(2)−S(4) 2.595(2), Cd(2)−S(5) 2.593(1), Cd(2)−O(3) 2.609(4), Cd(2)−O(4) 2.305(5), Cd(3)−S(5) 2.500(16), Cd(3)−S(6) 2.575(1), Cd(3)−S(7) 2.595(1), Cd(3)−O(5) 2.633(4), Cd(3)−O(6) 2.286(5), Cd(4)−S(7) 2.514(1), Cd(4)−O(7) 2.536(4), Cd(4)−S(8) 2.490(2), Cd(4)−O(8) 2.523(5), Cd(4)−S(2)#1 2.575(17). O(1)−Cd(1)−O(2) 155.74(17), O(1)−Cd(1)−S(1) 101.43(12), O(1)−Cd(1)−S(2) 84.78(11), O(1)−Cd(1)−S(3) 83.52(11), S(1)−Cd(1)−S(2) 122.61(7), S(1)−Cd(1)−S(3) 120.39(7), S(2)−Cd(1)−S(3) 117.00(5), O(2)−Cd(1)−S(1) 60.24(14), O(2)−Cd(1)−S(2) 117.97(13), O(2)−Cd(1)−S(3) 92.39(13), O(4)−Cd(2)−O(3) 80.0(2), O(4)−Cd(2)−S(3) 125.81(14), O(4)−Cd(2)−S(5)110.45(17), O(4)−Cd(2)−S(4) 61.45(17), S(3)−Cd(2)−S(5) 118.74(5), S(3)−Cd(2)−S(4) 124.13(6), O(6)−Cd(3)−O(5) 78.72(18), S(6)−Cd(3)−O(6) 62.76(15), O(6)−Cd(3)−S(5) 126.39(14), O(6)−Cd(3)−S(7) 110.61(6), S(6)−Cd(3)−S(5) 124.61(6), S(6)−Cd(3)−S(7) 102.33(6), S(5)−Cd(3)−S(7) 117.31(5), O(5)−Cd(3)−S(7) 82.21(11), O(5)−Cd(3)−S(6) 140.49(11), O(5)−Cd(3)−S(5) 84.63(10), O(8)−Cd(4)−O(7) 156.17(17), O(8)−Cd(4)−S(2)# 92.67(13), O(8)−Cd(4)−S(7) 118.04(14), O(8)−Cd(4)−S(8) 60.86(14), S(2)#−Cd(4)−S(7) 115.56(5), S(7)−Cd(4)−S(8) 123.25(7), S(2)#−Cd(4)−S(8) 121.19(7).

with a S_3CdO_2 core in which four coordination sites are occupied by one oxygen atom (O2) and one terminal and two bridging sulfur atoms (including two bridging ones) of thiophene-2-thiocarboxylate groups, while the fifth coordination site is occupied by the oxygen atom (O4) of a water molecule. From the angles subtended at Cd, τ was calculated to be 0.16, which suggests a slightly distorted square pyramidal geometry around the metal. S1, S3, O2, and O4 constitute the square plane, while S5 occupies the axial site. The Cd atom is tipped above the basal plane by 0.852 Å.

The Cd−O(4) bond length is comparable to the sum of the covalent radii of the two atoms (2.22 Å), while the Cd−O(2) bond is slightly longer and is comparable to the Cd−O distances observed in complexes **3a** and **3c**. The silver atom is at the center of a AgP_2S_2 core which is similar to those of **3a** and **3c**.

Complex **4** is a coordination polymer crystallized in a triclinic system with the space group $P\bar{1}$. The thermal ellipsoid plot is given in Figure 7.

It may be noted that besides the anionic cadmium thiobenzoate complexes there are only two structurally characterized neutral cadmium thiocarboxylate complexes: $[\{Cd(SCOPh)_2(\mu\text{-bpy})\}_n]$ and $[\{Cd_2(SCOPh)_4(\mu\text{-bpy})\}_n]$.[29] These compounds have one-dimensional polymeric structures. Interestingly, no neutral homoleptic thiocarboxylate compound of any group 12 metal has yet been characterized crystallographically.

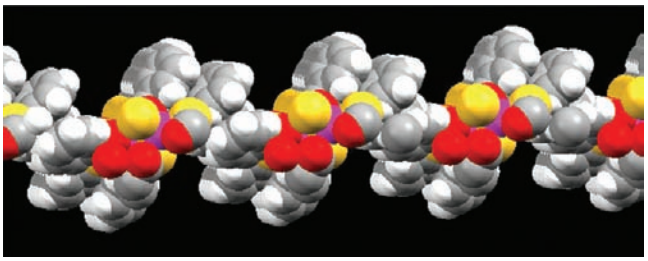

Figure 8. Helical structure of the polymeric chain of **4** along the *a* axis due to C···H_π interactions.

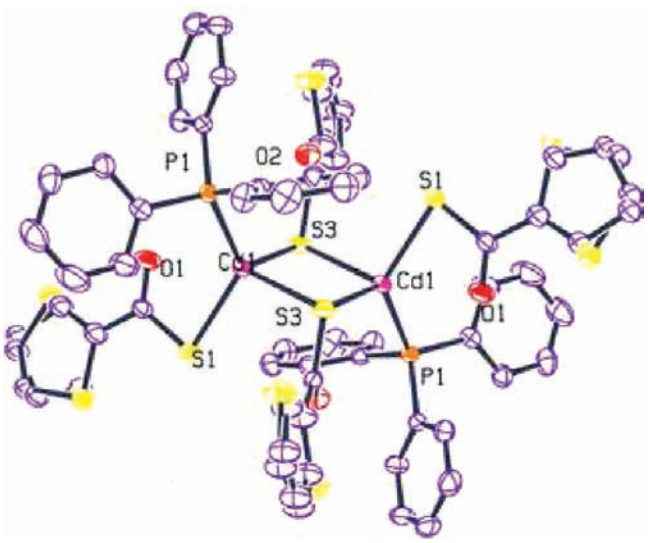

Figure 9. Thermal ellipsoid plot (at 30% probability level) of **5** with disordered thiophene rings (hydrogen atoms are omitted for clarity). Selected metric data: Cd(1)−S(1) 2.499(1), Cd(1)−$S(3)^{\#1}$ 2.552(14), Cd(1)−P(1) 2.576(1), Cd(1)−S(3) 2.725(1), S(3)−$Cd(1)^{\#1}$ 2.552(1), S(1)−Cd(1)−$S(3)^{\#1}$ 108.72(5), S(1)−Cd(1)−P(1) 123.60(4), $S(3)^{\#1}$−Cd(1)−P(1) 121.87(4), 101.83(4), $S(3)^{\#1}$−Cd(1)−S(3) 97.44(3), P(1)−Cd(1)−S(3) 95.11(4), $Cd(1)^{\#1}$−S(3)−Cd(1) 82.56(3).

In a polymeric chain (Figure SI-1; Supporting Information), each Cd atom is chelated by one thiobenzoate ligand, while one oxygen and two sulfur atoms from three different ligands occupy three coordination sites in a five-coordinate environment. Each carbonyl oxygen of the bridging ligands is also bonded to another Cd center. A closer look at the coordination environments around the Cd atoms revealed that there are two different types of Cd(II) centers. The coordination spheres around Cd1 and Cd4 are identical, while those around Cd2 and Cd3 are of a different kind.

The orientations of the chelating ligands around Cd1 and Cd3 are shown schematically in Figure 7. Cd1 possesses a distorted trigonal bipyramidal environment (τ = 0.72) made by two oxygen and three sulfur atoms. The sulfur atoms occupy the vertices of the equatorial plane forming an approximately equilateral triangle. The Cd1 atom lies in the S3 plane. The O1 sits rather perfectly on one of the axial sites (O1−Cd1−S angles varying between 83.52 and 101.42°), while the other oxygen O2 is highly displaced from the ideal axial position because of the small bite angle of the SCO unit.

The geometry around Cd3 is different, basically because of the altered orientation of the chelating thiobenzoate ligand. Moreover, the Cd3−O6 distance is quite short. As a result, the geometry around Cd3 (τ = 0.23) is closer to that of a square pyramid. The Cd3 atom is displaced from the S_2O plane (by 0.346 Å). The angles between Cd−S bonds (102.33 and 124.61°) are far away from 90°. In view of these distortions, an alternative description could also be made considering the environment around Cd3 to be closer to a tetrahedron having S7, S5, S6, and O6 at the vertices, while the O5 atom caps the triangular S7S6O6 face. Expectedly, the Cd3−O5 distance is larger than the Cd1−O1 distance.

Table 2. Bond-Valence Parameters for 1, 3a, and 3c

complex	Cd−S (Å)		Cd···O (Å)		total bond valency (V_i)	ratio of Cd···O/ Cd−S
1	Cd−S1	2.548	Cd−O1	2.560	2.07	0.43
	Cd−S2	2.565	Cd−O2	2.487		
	Cd−S3	2.610	Cd−O3	2.431		
3a	Cd−S1	2.613	Cd−O1	2.464	2.06	0.33
	Cd−S3	2.475	Cd−O2	2.650		
	Cd−S5	2.572	Cd−O3	2.579		
3c	Cd−S1	2.577	Cd−O1	2.541	2.07	0.32
	Cd−S2	2.584	Cd−O2	2.542		
	Cd−S3	2.477	Cd−O3	2.623		

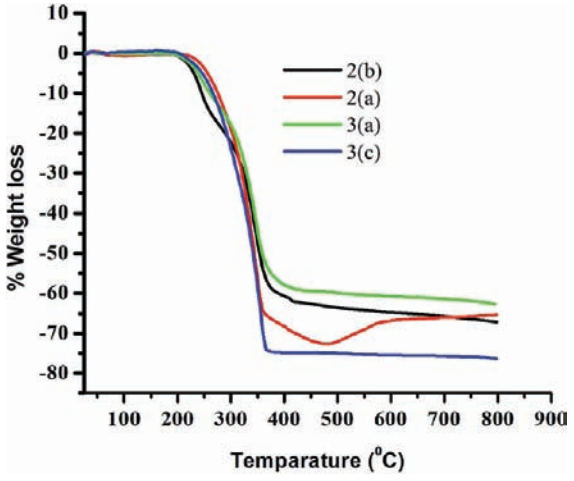

Figure 10. Thermal decomposition patterns of complexes **2a**, **2b**, **3a**, and **3c**.

Due to C···H π interactions (2.88 Å), the polymeric chain has a helical structure along the *a* axis (Figure 8).

Complex **5** is a symmetrical homobimetallic complex with a $PSCd(\mu\text{-}S)_2CdSP$ core (Figure 9). In this molecule, each Cd center is primarily bonded to a phosphorus atom of the triphenyl phosphine ligand and the sulfur atoms of three thiophene-2-thiocarboxylate ligands acquiring a distorted trigonal pyramidal geometry (τ_4 = 0.81). The Cd atom is displaced from the basal plane constituted by P1, S1, and one of the bridging S atoms by 0.355 Å. The two M−S bonds are nonequivalent, which is a usual feature observed in complexes with a Cu_2S_2 core.[30] As the oxygen (O1) of the terminal thiophene thiocarboxylate group is very close to the Cd atom (at a distance of 2.674 Å), an alternative description of the structure could be made, including O1 in the coordination sphere, thus imparting a highly distorted distorted trigonal bipyramidal geometry (τ = 0.60) around the Cd(II) center.

Total Bond Valence Approach. Vittal et al.[22] have calculated bond-valence parameters[31,32] for the anionic zinc and cadmium thiobenzoate complexes. Similar calculations have been performed on the complexes **1**, **3a**, and **3c** [about CdS_3O_3 units in complexes]. In all of these cases, the ratio of contributions of Cd···O to Cd···S are higher than those in the earlier reported anionic complexes, revealing the significance of Cd···O bonds. The calculated bond valence parameters are given in Table 2.

Electronic Absorption Spectra. Electronic absorption spectra of all of the heterobimetallic complexes were recorded as their chloroform solutions (2×10^{-3} M). For complex **1**, the spectrum was recorded as a DMSO solution.

The electronic absorption spectra of the complexes of thiophene-2-thiocarboxylate are comparable with one another. Complex **1** showed a broad absorption band at 417 nm and sharp peaks with comparatively higher intensities in the higher energy region at 291, 246, and 219 nm (Figure SI2; Supporting Information). It may be noted that only two strong intensity peaks (at 311 and 260 nm) were observed in the spectrum of the sodium salt of the ligand. The appearance of a peak at the lower energy region (417 nm) in **1** was possibly due to the $n \rightarrow \pi^*$ intraligand and metal to ligand charge transfers.

Complex **2b** (Figure SI3; Supporting Information) showed a broad absorption band at 421 nm due to the metal to ligand charge transfers and two other intense absorptions at 324 and 250 nm assignable to the intraligand charge transfers. In the case of **3a** (Figure SI 4, Supporting Information), the sharp absorptions at 332, 300, and 253 nm may be assigned as intraligand/interligand charge transfer bands. However, in **3b** (Figure SI 4, Supporting Information), lower energy absorption bands at 492 and 456 nm possibly arose due to the charge transfers involving the electron pairs of the oxygen of coordinated water.

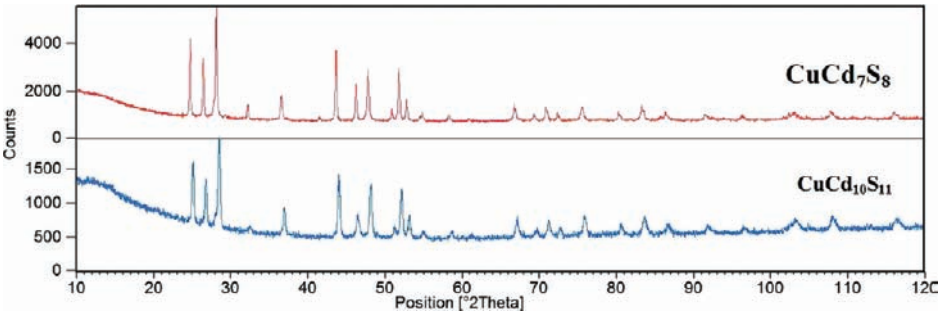

Figure 11. PXRD patterns of **6** and **7**.

dx.doi.org/10.1021/ic200927w |*Inorg. Chem.* 2011, 50, 10056–10069

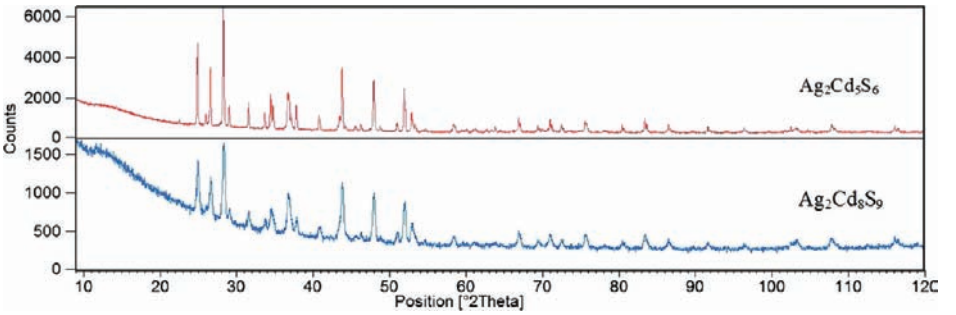

Figure 12. PXRD patterns of **8** and **9**.

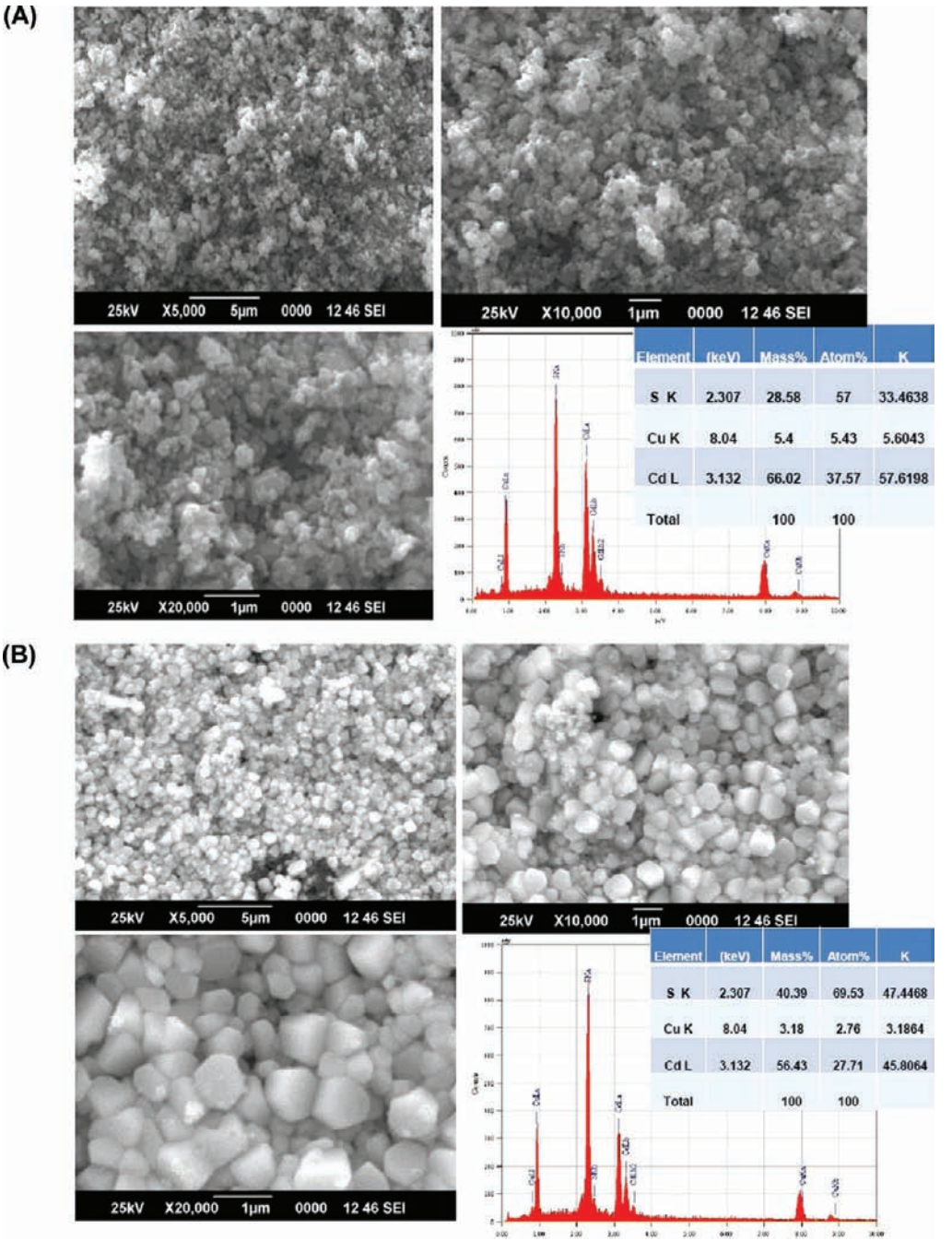

Figure 13. SEM-EDS images of (A) **6** and (B) **7**.

dx.doi.org/10.1021/ic200927w |*Inorg. Chem.* 2011, 50, 10056–10069

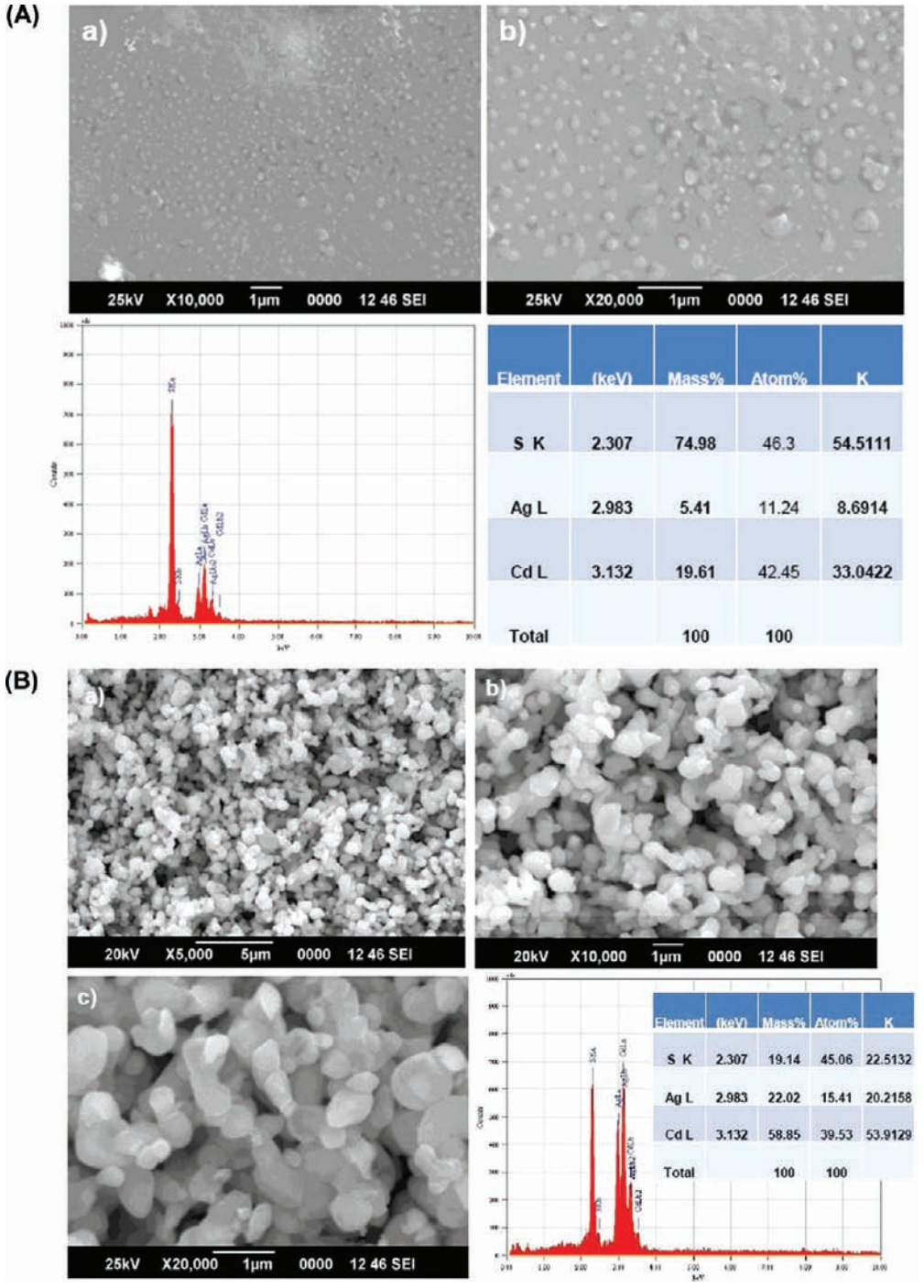

Figure 14. SEM-EDS images of (A) **8** and (B) **9**.

In the case of **2a** (Figure SI3; Supporting Information), the electronic absorption spectrum (in solid state) showed peaks at 250 and 299 nm assignable as intraligand charge transfer bands, whereas the peak at 375 nm was possibly due to the metal to ligand charge transfer. In solution, a broad peak covering 299−400 nm is observed beside the one at 250 nm. In the spectrum of **3c** (Figure SI3, Supporting Information), peaks observed at 338 and 317 nm may be due to the intraligand/interligand charge transfers, while the peaks at higher energy absorption bands 244 and 220 nm may be assigned as intraligand charge transfers.

In the solid state spectrum (Figure SI5, Supporting Information) of **4**, strong intensity peaks were observed at 249 and 269 nm, while two peaks with lower intensities were observed at 395 and 423 nm. The strong intensity peaks were expected to be due to the intraligand charge transfers, whereas the lower intensity peaks observed at lower frequencies may have arisen possibly due to the metal to ligand charge transfers.

Thermogravimetry and Pyrolysis. We have investigated the thermal decomposition patterns of the Cd/Cu- and Cd/Ag-containing thiocarboxylate complexes **2a**, **2b**, **3a**, and **3c** (Figure 10). Complexes **2a**, **2b**, **3a**, and **3c** showed single step decomposition in

dx.doi.org/10.1021/ic200927w |*Inorg. Chem.* 2011, 50, 10056–10069

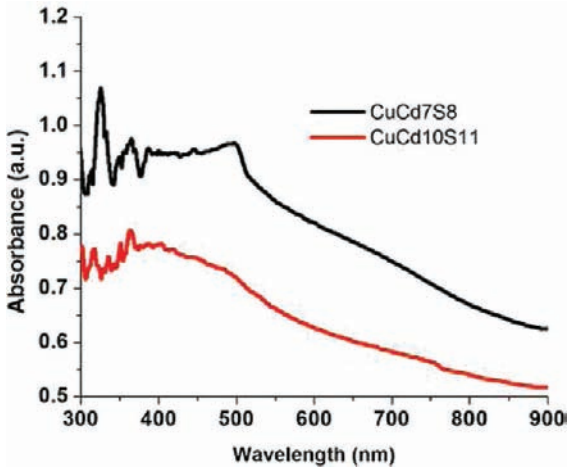

Figure 15. Absorption spectra of **6** and **7** in the solid state (recorded as Nujol mulls).

the TGA experiment. In the case of **2a**, decomposition occurred in the temperature range of 221−369 °C with a 65% weight loss, whereas for sulfur-rich complex **2b**, decomposition was observed between 200 and 395 °C with a 61% weight loss. Complex **3a** showed a one-step decomposition in the temperature range of 200−415 °C with a 58% weight loss; however, **3c** showed a 74.62% weight loss in the temperature range 192−372 °C. From the residual weights of the pyrolyzed products, it is not possible to predict their elemental composition. However, the higher residual weights in the cases of **2b** and **3a** indicate higher percentages of sulfur which have originated from the presence of an extra sulfur atom in each thiophene-2-thiocarboxylate ligand. Earlier studies on thermal decomposition of a few thiocarboxylate complexes have shown that metal sulfides are the end products of pyrolysis.[12,21] Our recent experiments on the pyrolysis of Pb/Cu and Pb/Ag heterobimetallic complexes resulted in the corresponding bimetallic oxides.[33]

On the basis of these TGA results, we have performed pyrolysis experiments. On pyrolyzing the complexes **2a** and **2b**,

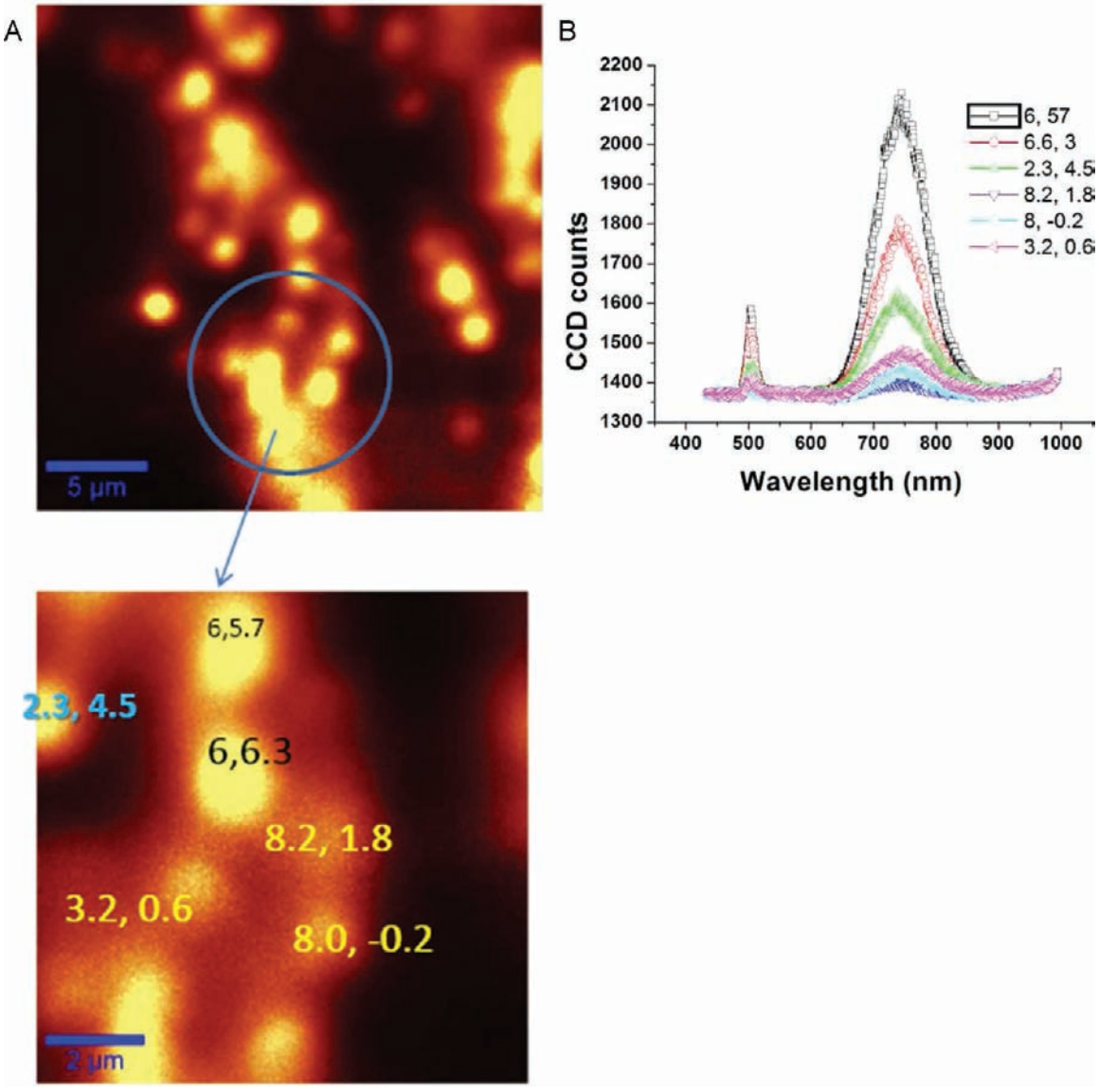

Figure 16. (A) Confocal micrographs of the regions from where PL spectra were recorded. (B) Photoluminescence spectra of **6** (λ_{exc} = 488 nm at an excitation power of 0.1 mW).

dx.doi.org/10.1021/ic200927w |*Inorg. Chem.* 2011, 50, 10056–10069

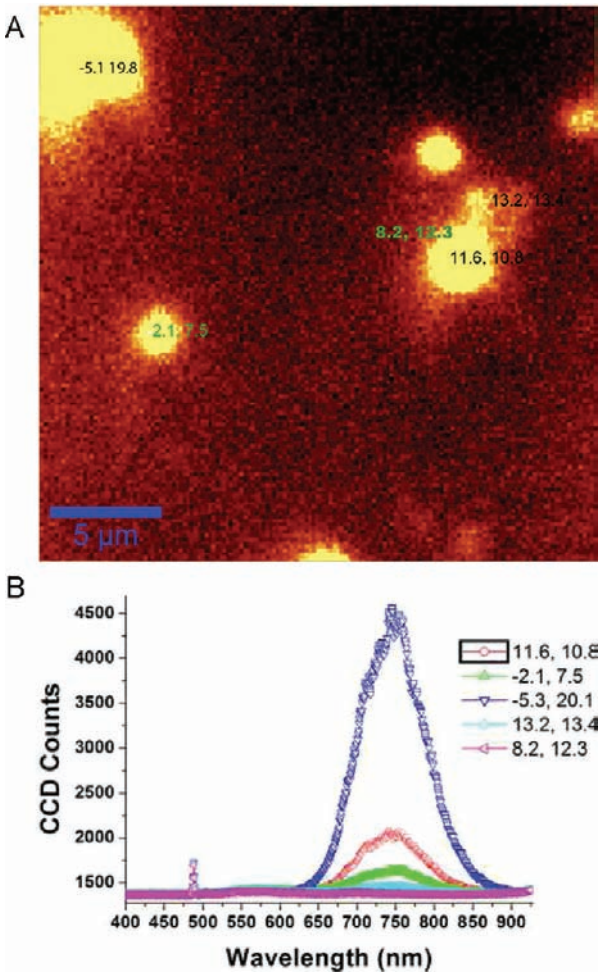

Figure 17. (A) Confocal micrograph of surface area used for data collection. (B) PL spectra of **7** (λ_{exc} = 488 nm at excitation power 0.3 mW).

ternary sulfide products $CuCd_7S_8$ (**6**) and $CuCd_{10}S_{11}$ (**7**) were isolated, respectively. Similarly, after pyrolysis of the Ag/Cd-containing complexes **3a** and **3c**, $Ag_2Cd_8S_9$ (**8**) and $Ag_2Cd_5S_6$ (**9**) were isolated, respectively. (The compositions are based on the ratio of the two metals found by EDX spectral analyses.)

Nature of the Sulfide Particles. The metal sulfides were studied through their powder X-ray diffraction patterns (Figures 11 and 12). In both (**6** and **7**) cases, reflections of CdS (greenockite, JCPDS No. 00−02−0563) and CuS (covellite, JCPDS No. 01−075−2235) are clearly observed. On first sight, it appears that the product is a mixture of CdS and CuS; however, a closer look into the diffraction pattern revealed small changes in *d*-spacings with respect to pure greenockite. Such a pattern is indicative of a solid solution formation (alloying).[34,35] The peak observed at a *d*-spacing of 3.12 Å in greenockite (hexagonal CdS) showed a shift to larger values of 3.16 and 3.17 Å, respectively, in **6** (10% Cu) and **7** (14.2% Cu; Table SI 1, Supporting Information). Variations in lattice parameters are obviously small in these cases.[36] Earlier studies on copper−cadmium sulfides prepared by coprecipitation led to the formation of two separate mineral phases (CuS and CdS), and the X-ray diffraction spectra showed reflections due to both pure phases.[37]

In the X-ray diffraction spectra of the pyrolysis products of **3a** and **3c** (Figure 12), reflection peaks of greenockite (JCPDS No. 00−02−0563) and acanthite (Ag_2S, JCPDS No. 01−003−0844) are noticeable. As observed in **6** and **7**, the *d*-spacings in **8** and **9** (Table SI2; Supporting Information) also showed small changes [the *d* value of 3.12 Å (for 101 peak of pure CdS) shifted to 3.15 and 3.17 Å in **8** and **9**, respectively], indicating the formation of homogeneous solid solutions of metal sulfides $Ag_2Cd_8S_9$ and $Ag_2Cd_5S_6$. To the best of our knowledge, no silver−cadmium sulfides have ever been reported.

Surface Morphology. The surface morphologies of **6** and **7** were studied using scanning electron microscopy (Figure 13), which showed the presence of uniform granular crystallites. Notably, the earlier reported $(CuS)_x(CdS)_{1-x}$ showed distinct CuS and CdS phases in the scanning electron micrographs.[37] Figure 14 shows the SEM topography of **8** and **9**. At 10 000 magnifications, the surface image of **9** looks granulated with irregular sizes and shapes; however, **8** has a uniform blistered surface which bears no cracks.

Optical Properties. The optical properties of **6** and 7 were investigated by UV−visible spectra, as shown in Figure 15. In both cases, due to the presence of copper, the electronic absorption spectra showed a shift toward longer wavelengths in comparison to the CdS, which covers only the ultraviolet absorption range from 310 to 490 nm.

Photoluminescence and Photoluminescence Excitation Spectra. The PL spectra of **6** and **7** confirmed the compositional homogeneity of the sample. The spectral pattern remained unchanged over the whole film of the sample, and the intensities varied with the film thickness proportionately, which could be monitored by confocal microscopy. The higher energy band edge emission with a narrow fwhm (12 nm) was observed at 504 nm, while the lower energy Cu dopant emission appeared as a broad and intense peak centered at 745 nm (86 nm fwhm). It may be mentioned here that the band edge emission of CdS/CdSe nanocrystallites is usually more intense than the lower energy deep trap emission band which appears at >700 nm[35] The Cu dopant emission on the other hand has a higher intensity and is more red-shifted.[14] Figure 16a indicates the surface region from where the PL spectra were recorded.

Intensities of emission peaks in the spectrum of **7** (Figure 17) were very poor compared to those obtained in **6** under identical conditions (λ_{exc}: 488 nm, 0.1mW, integration time 5 s) due to the comparatively low copper content in it as compared to **6**. However, when excitation power was increased from 0.1 to 0.3 mW, the number of CCD counts enhanced appreciably. The band edge emission was observed at 499 nm (fwhm = 2 nm), while the Cu dopant emission was found at 745 nm (fwhm = 92 nm). Interestingly, the deep trap emission of CdS was also observable as a weak intensity band centered at 573 nm (fwhm = 175 nm).

The band edge emissions are red-shifted from the band edge absorption peak by 16 and 11 nm, respectively, in **8** and **9**. These shifts can be corroborated with the quantities of CuS in the CdS solvent.

Pressed Pellet Electrical Conductivity. For the complex $[Cd(SCOPh)_2]_n$, electrical conductivity data were recorded from 309 to 353 K, while in case of ternary metal sulfides, the conductivity data were collected from 303 to 493 K.

At room temperature (36 °C), the $[Cd(SCOPh)_2]_n$ polymer showed an electrical conductivity of 1.56×10^{-7} S/cm, which deceased with a rise in temperature, and at 80 °C, it became nonconducting ($\sigma = 1.75 \times 10^{-11}$ S/cm). The decrease in electrical conductivity with an increase in temperature indicates

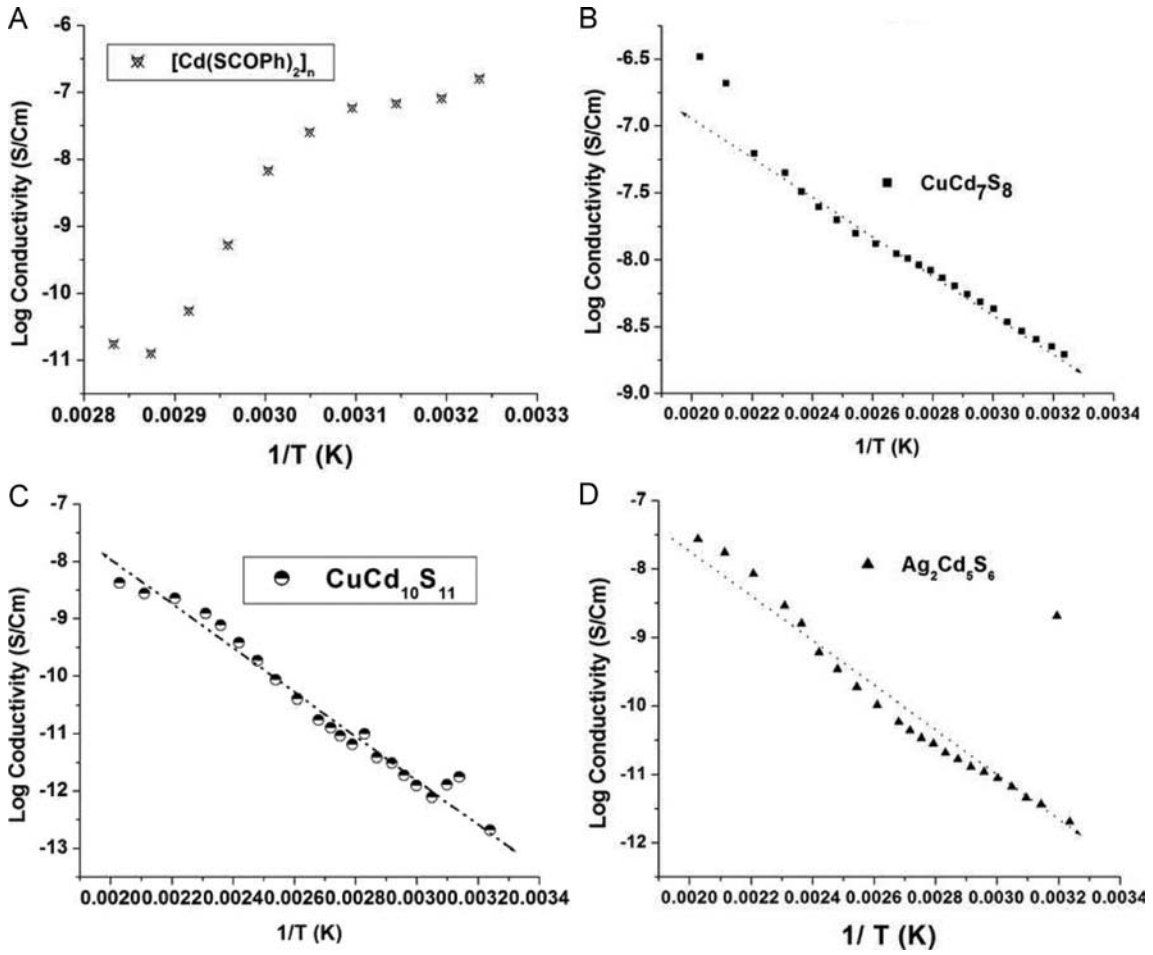

Figure 18. Pressed pellet electrical conductivities of (A) **4**, (B) **6**, (C) **7**, and (D) **9**.

that the $[Cd(SCOPh)_2]_n$ polymer has a metal-like conducting nature (Figure 18a).

The room temperature electrical conductivity of the ternary metal sulfides of Cd/Cu are comparable to each other. In the case of $CuCd_7S_8$, the room temperature pressed pellet electrical conductivity was 1.63×10^{-9} S/cm at 36 °C, which gradually increased to 3.28×10^{-7} S/cm at 220 °C (Figure 18b), while in the case of $CuCd_{10}S_{11}$, the room temperature electrical conductivity was 2.08×10^{-13} S/cm, which continuously increased with the temperature. Finally, at 220 °C, it became 4.20×10^{-9} S/cm. (Figure 18c).

Silver-containing ternary metal sulfide $Ag_2Cd_5S_6$ showed a pressed pellet electrical conductivity of 2.03×10^{-12} S/cm at room temperature (36 °C), which gradually increased to 2.70×10^{-8} S/cm at 220 °C, indicating its semiconducting nature (Figure 18d).

CONCLUSION

We have synthesized and structurally characterized novel heterobimetallic Cd(II)/Cu(I) and Cd(II)/Ag(I) thiocarboxylate complexes along with a polymeric Cd(II) thiobenzoate. The compounds of Cd(II)/Ag(I) are unique, being the first ones containing these two metal atoms in the same molecule. The heterobimetallic complexes on pyrolysis yielded corresponding ternary sulfides. Unlike the products of earlier attempts, these sulfides are solid solutions of CuS in CdS. While the Ag/Cd sulfides are the first ones of their kind. Thus, this study provides a low energy pathway for making copper or silver doped CdS nanoparticles.

ASSOCIATED CONTENT

Supporting Information. Additional figures and crystallographic information files (CIF). This material is available free of charge via the Internet at http://pubs.acs.org.

AUTHOR INFORMATION

Corresponding Author

*E-mail: s_bhatt@bhu.ac.in.

Author Contributions

§J.C. and S.S. have equal contributions in this paper

ACKNOWLEDGMENT

The authors are grateful to Prof. T. N. Guru Row, S.S.C.U., Indian Institute of Science, for powder X-ray diffraction measurements; Dr. Jaydeep Basu and Mr. Laxmi Narayan Tripathi, Department of Physics, Indian Institute of Science, Bangalore for PL measurements; Director, SAIF, Cochin, India for SEM-EDX studies; and Prof. R. S. Tiwari, Physics Department, Banaras Hindu University for useful discussions. Financial assistance to

S.B. in the form of a scheme and fellowships to J.C. and S.S. by the Council of Scientific and Industrial Research, India are gratefully acknowledged.

REFERENCES

(1) (a) Wang, Q.; Xu, Z.; Yin, H.; Nie, Q. *Mater. Chem. Phys.* **2005**, *90*, 73. (b) Wang, Y. *Acc. Chem. Res.* **1991**, *24*, 133.(c) Mönch, W. *Semiconductor Surfaces and Interfaces*, 3rd ed.; Springer-Verlag: Berlin, 2001; p 105. (d) Vanderah, T. A. *Chemistry of Superconductor Materials, Preparation, Chemistry, Characterization and Theory*; Noyes Publication: Park Ridge, NJ, 1992; p 23. (d) Chander, H. *Proc. ASID* **2006**, 11. (e) Dance, I. *Chem. Aust.* **1997**, 38. (e) Sriram, M. A.; Kumta, P. N. *J. Mater. Chem.* **1998**, *8*, 2441.

(2) Rakshani, A. E.; Pradeep, B. Ramazaniyan, H. A. In *Chemical Solution Deposition of Semiconducting and Non-Metallic Films*; Lincot, D, Hodes, G., Ed.; Electrochemical Society Inc.: Pennington, NJ, 2006; p 49.

(3) Minkus, W. *Phys. Rev.* **1965**, *138*, A1277.

(4) (a) Garg, H. P. *Adv. Solar Energy Tech.* **1987**, *3*, 366. (b) Reynolds, D.; Leies, G.; Antes, L.; Marburger, R. *Phys. Rev.* **1954**, *96*, 533.

(5) Fouassier, C. *Luminescence in Encyclopedia of Inorganic Chemistry*; John Wiley: New York, 1994.

(6) Van der Put, P. J. *The Inorganic Chemistry of Materials*; Plenum Press: New York, 1998; p 273.

(7) Vittal, J. J.; Deivaraj, T. C. *Progr. Crystal Growth Charact. Mater.* **2002**, *45*, 21.

(8) (a) O'Brien, P. Pickett, N. L. In *Comprehensive Coordination Chemistry II*; McCleverty, J. A., Meyer, T. J., Eds.; Elsevier: Oxford, U.K., 2004; Vol. 9, p 1005. (b) O'Brien, P. Pickett, N. L. In *Chemistry of Nanomaterials*; Rao, C. N. R., Mueller, A., Cheetham, A. K., Eds.; Wiley-VCH Verlag GmbH & Co. KGaA: Weinheim, Germany, 2004; Vol. 1, p 12.

(9) Malik, M. A.; Afzaal, M.; O'Brien, P. *Chem. Rev.* **2010**, *110*, 4417.

(10) (a) Singh, P.; Bhattacharya, S.; Gupta, V. D.; Nöth, H. *Chem. Ber* **1996**, *129*, 1093. (b) Singh, S.; Chaturvedi, J.; Bhattacharya, S.; Nöth, H. *Polyhedron* **2011**, *30*, 93.

(11) Nyman, M. D.; Hampden-Smith, M. J.; Duesler, E. N. *Inorg. Chem.* **1997**, *36*, 2218.

(12) Vittal, J. J.; Ng, M. T. *Acc. Chem. Res.* **2006**, *39*, 869 and references therein.

(13) (a) Yang, Y.; Chen, O.; Angerhofer, A.; Cao, Y. C. *J. Am. Chem. Soc.* **2006**, *128*, 12428. (b) Xie, R.; Peng, X. *J. Am. Chem. Soc.* **2009**, *131*, 10645. (c) Vlaskin, V. A.; Janssen, N.; Rijssel, J. V.; Beaulac, R.; Gamelin, D. R. *Nano Lett* **2010**, *10*, 3670. (d) Zeng, R.; Rutherford, M.; Xie, R.; Zou, B.; Peng, X. *Chem. Mater.* **2010**, *22*, 2107. (e) Acharya, S.; Sarma, D. D.; Jana, N. R.; Pradhan, N. *J. Phys. Chem. Lett.* **2010**, *1*, 485. (f) Martyshkin, D. V.; Fedorov, V. V.; Kim, C.; Maskalev, I. S.; Mirov, S. B. *J. Opt.* **2010**, *12*, 024005. (g) Pradhan, N.; Peng, X. *J. Am. Chem. Soc.* **2007**, *129*, 3339. (h) Jana, S.; Srivastava, B. B.; Acharya, S.; Santra, P. K.; Jana, N. R.; Sarma, D. D.; Pradhan, N. *Chem. Commun.* **2010**, *46*, 2853. (i) Srivastava, B. B.; Jana, S.; Karan, N. S.; Paria, S.; Jana, N. R.; Sarma, D. D.; Pradhan, N. *J. Phys. Chem. Lett.* **2010**, *1*, 1454. (j) Pradhan, N.; Goorskey, D.; Thessing, J.; Peng, X. *J. Am. Chem. Soc.* **2005**, *127*, 17586.

(14) Srivastava, B. B.; Jana, S.; Pradhan, N. *J. Am. Chem. Soc.* **2011**, *131*, 1007.

(15) Furniss, B. S.; Hannaford, A. J.; Smithand, P. W. G. Tatchell, A. R.; *Vogel's Textbook of Practical Organic chemistry*, 5th ed.; Dorling Kindersley: India, 2006.

(16) Singh, S.; Bhattacharya, S.; Nöth, H. *Eur. J. Inorg. Chem.* **2010**, 5691.

(17) *CrysAlis Pro*; Agilent Technologies: Yamton, England, 2010.

(18) Sheldrik, G. M. *SHELX 97*; University of Gottingen: Gottingen, Germany, 1997.

(19) Farrugia, L. J. *J. Appl. Crystallogr.* **1999**, *32*, 837.

(20) Vinogradova, E. A.; Vassilyeva, O. Y.; Kokozay, V. N.; Skelton, B. W.; Bjernemose, J. K.; Raithby, P. R. *J. Chem. Soc., Dalton Trans.* **2002**, 4248.

(21) Singh, S.; Chaturvedi, J.; Aditya, A. S.; Reddy, N. R.; Bhattacharya, S. Unpublished results.

(22) (a) Vittal, J. J.; Dean, P. A. W. *Inorg. Chem.* **1996**, *35*, 3089. (b) Dean, P. A. W.; Vittal, J. J.; Craig, D. C.; Scudder, M. L. *Inorg. Chem.* **1998**, *37*, 1661.

(23) Addison, A. W.; Rao, T. N.; Reedijk, J.; Rijn, J.; van and Verschoor, G. C. *J. Chem. Soc., Dalton Trans.* **1984**, 1349.

(24) (a) Deivaraj, T. C.; Lai, G. X.; Vittal, J. J. *Inorg. Chem.* **2000**, *39*, 1028. (b) Singh, S.; Chaturvedi, J.; Bhattacharya, S. *Dalton Trans.* **2011** DOI: 10.1039/C1DT10629E.

(25) Yang, L.; Powell, D. R.; Hoser, R. F. *Dalton Trans* **2007**, 955.

(26) (a) Vittal, J. J.; Dean, P. A. W. *Inorg. Chem.* **1993**, *32*, 791. (b) Deivaraj, T. C.; Dean, P. A. W.; Vittal, J. J. *Inorg. Chem.* **2000**, *39*, 3071.

(27) Deivaraj, T. C.; Park, J.-H.; Afzaal, M.; O'Brien, P.; Vittal, J. J. *Chem. Mater.* **2003**, *15*, 2383.

(28) Deivaraj, T. C.; Vittal, J. J. *J. Chem. Soc., Dalton Trans.* **2001**, 329.

(29) Vittal, J. J.; Sampanthar, J. T.; Lu, Z. *Inorg. Chim. Acta* **2003**, *343*, 224.

(30) (a) Casas, J. S.; Castellano, E. E.; Couce, M. D.; Garćia-Vega, M.; Śanchez, A.; Śanchez-Gonźalez, A.; Sordo, J.; Varela, J. M.; Vázquez Lópe z, E. M. *Dalton Trans.* **2010**, *39*, 3931. (b) Fang, H.-C.; Yi, X.-Y.; Gu, Z.-G.; Zhao, G.; Wen, Q.-Y.; Zhu, J.-Q.; Xu, A.-W.; Cai, Y.-P. *Cryst. Grow. Des.* **2009**, *9*, 3776. (c) Fernández, P.; Sousa-Pedrares, A.; Romero, J.; García-Vázquez, J. A.; Sousa, A.; Pérez-Lourido, P. *Inorg. Chem.* **2008**, *47*, 2121.

(31) Altermatt, D.; Brown, I. D. *Acta Crystallogr.* **1985**, *B41*, 240.

(32) Brown, I. D.; Altermatt, D. *Acta Crystallogr.* **1985**, *B41*, 244.

(33) Chaturvedi, J.; Bhattacharya, S.; Prasad, R. *Dalton Trans* **2010**, *39*, 8725.

(34) Denton, A. R.; Ashcroft, N. W. *Phys. Rev.* **1991**, *A43*, 3161.

(35) (a) Swafford, L. A.; Weigand, L. A.; Bowers, M. J., II; McBride, J. R.; Rapport, J. L.; Watt, T. L.; Dixit, S. K.; Feldman, L. C.; Rosenthal, S. J. *J. Am. Chem. Soc.* **2006**, *128*, 12299. (b) Smith, D. K.; Luther, J. M.; Semonin, O. E.; Nozik, A. J.; Beard, M. C. *ACS Nano* **2011**, *1*, 183.

(36) Jarabek, B. R.; Grier, D. G.; Simonson, D. L.; Seidler, D. J.; Boudjouk, P. McCarthy, G. J. JCPDS—International Centre for Diffraction Data; Newtown Square, PA, 1997.

(37) Tsamouras, D.; Dalas, E.; Sakkopoulos, S.; Koutsoukos, P. G. *Langmuir* **1999**, *15*, 8018.